The Electrocatalytic Activity of Pyrazolyl-thioimidazolyl borate-based Zinc(II) Complexes Towards the Hydrolysis of Tris(*p*-nitrophenyl)phosphate

Gaber A. M. Mersal[1,2,*], Mohamed M. Ibrahim[1,3], Sahar Fadllalh[1,4], Hamdy S. El-Sheshtawy[3], Mona M. B. Al-Malki[1]

[1] Chemistry Department, Faculty of Science, Taif University, 888 Taif, KSA.
[2] Chemistry Department, Faculty of Science, South Valley University, Qena, Egypt
[3] Chemistry Department, Faculty of Science, Kafr El-Sheikh University, Kafr El-Sheikh 33516, Egypt.
[4] Chemistry Department, Faculty of Science, Cairo University, Egypt
[*]E-mail: gamersal@yahoo.com

Two zinc(II) compounds of pyrazolyl-thioimidazolyl containing ligands of the types $[HB(Pz^{MePh})(Tt^{OMe})_2ZnCl]$ **1** and $[HB(Pz^{MePh})(Tt^{OMe})_2ZnClO_4]$ **2** were synthesized and characterized as new electrocatalysts for the hydrolysis of the phosphotriester tris(*4*-nitrophenyl)phosphate (TPP). Their structures were characterized spectroscopically by infrared and ^1H-^{13}C NMR spectroscopies as well as elemental analysis and thermal analysis. The zinc atoms adopt distorted tetrahedral geometry with coordination chromophores ZnS_2NCl and ZnS_2NO for complexes **1** and **2**, respectively. The electrochemical behavior of the obtained zinc complexes-modified carbon paste electrode (Zn-CPE) has been studied by cyclic voltammetry. The Zn-CPE shows good electrocatalytic activities toward the hydrolysis of TPP, generates the oxidized *p*-nitrophenol at the surface of CPE. Several parameters were investigated to evaluate the performance of the biomimetic sensor obtained after the incorporation of zinc(II) complexes **1** and **2** in a carbon paste electrodes.

1. INTRODUCTION

The importance of insecticides to defeat bacteria is increasing through the time. This was due to the excessive agriculture activities, which is the main source of the insecticides residues in food, soil, and water. Insecticides are substances which used to kill defeat a harmful insects. The increase in

agricultural production increases the level of insecticide residues in foodstuff, soil and water [1]. To avoid the side effects of the insecticides, systematic control for the residues remains in agricultural products, food, soil and water is required. For example, determination of toxic *p*-nitrophenol level in different environmental samples is essential. *p*-nitrophenols formed as a result for the degradation of different organophosphorous pesticides such as parathion and fenitronthion [2,3].

The ability of metal complexes to catalysis the hydrolysis reaction of neutral tetrahedral phosphorus centers was extensively discussed [4-10]. In the hydrolysis process, the phosphorus complexes degrade the toxic materials. The mechanism of the interactions between zinc (II) ions and phosphorus esters compounds was widely studied [10-12]. For example, mononuclear zinc (II) complexes, which are structurally and functionally mimicking the active site of *phosphotriestrase,* and phosphorus esters compounds, are designed and examined towards the hydrolysis of the toxic organophophosphate according to the following Scheme 1 [13-16].
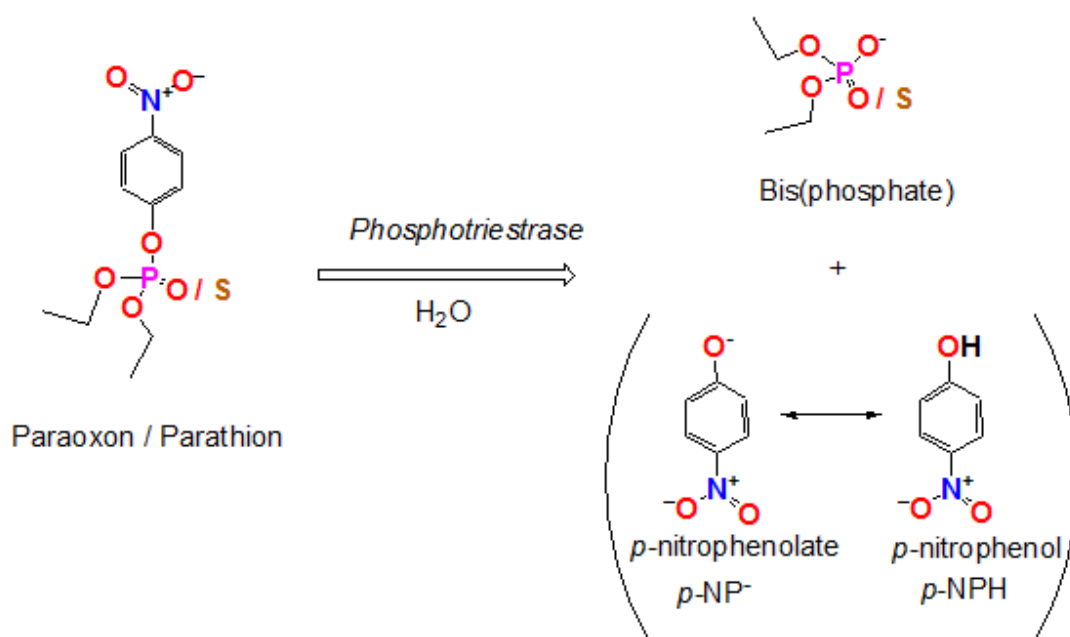
Scheme 1. The hydrolysis reaction of the toxic organophosphates by the action of *phosphotriestrase*

In continuation to our ongoing study on the biomimetic/duplication of *hydrolase enzyme* and the degradation of toxic organophospates (Ops) [4,5], the present study is based on electroanalytical techniques through the development and application of a new artificial biosensors [17-19] for the determination of TPP as a structural mimic for the toxic OPs. The artificial biomimetic sensors were prepared by mixing a graphite powder with a hot paraffin wax in the presence of the ligand $K[HB(Pz^{MePh})(Tt^{OMe})_2]$ and its zinc(II) complexes $[HB(Pz^{MePh})(Tt^{OMe})_2ZnCl]$ **1** or $[HB(Pz^{MePh})(Tt^{OMe})_2ZnClO_4]$. The electrochemical behavior of TPP on the prepared biomimetic sensor has been investigated by using cyclic and square wave voltammetry. The effect of different experimental parameters such as type of supporting electrolyte, pH, deposition potential, accumulation time and different square wave voltammetric parameters has also been investigated on the peak height

of parathion. The effect of some interference due to the presence of other organic compounds on the peak height of TPP will be studied. The zinc(II) model complexes catalyzed the hydrolysis of OPs with nitrophenyl substituent to generate *p*-nitrophenol, which, is electrochemically oxidized at carbon paste working electrode at fixed potential as a function of pH *vs* reference electrode to generate a current that is proportional to the pesticide concentration.

2. EXPERIMENTAL

2.1 Materials and methods

The zinc(II) salts were obtained from Sigma-Aldrich, Germany. The phosphotriester tris(*4*-nitrophenyl)phosphate (TPP) was obtained from Hokkaido University, Sapporo, Japan. The ligand, potassium hydro{bis(3-methyl-5-phenylpyrazolyl)1-anizylthioimidazolyl}borate [KHB(Pz^{MePh})-(Tt^{OMe})$_2$] and its zinc(II) complexes **1** and **2** were synthesized according to literature [20-23]. Infrared spectral measurements were recorded using Alpha-Atunated FT-IR Spectrophotometer, Bruker in the range of 400-4000 cm^{-1}. ^{1}H NMR spectra were monitored using Varian 400-NMR spectrophotometer, employing TMS as a reference and DMSO-d$_6$ as a solvent. Thermal analysis measurement was done on Netzsch STA 449F3 in an atmosphere of nitrogen.

2.2 Synthesis of Zinc complexes

2.2.1. Synthesis of {[HB(Pz^{MePh})(Tt^{OMe})$_2$]ZnCl} 1

A solution of K[HB(Pz^{MePh})(Tt^{OMe})$_2$] (618 mg, 1.0 mmol) in 50 mL of MeOH was added drop wise (30 min) to a solution of anhydrous ZnCl$_2$ (150 mg, 1.1 mmol) in methanol (30 mL). The resulting precipitate was filtered off. The filtrate was reduced to 20 mL, producing a white precipitate, washed with ether, and finally dried under vacuum. Anal. for C$_{30}$H$_{28}$BClN$_6$O$_2$S$_2$Zn (618.62): Calcd.: C, 52.96; H, 4.15; N, 12.35; S, 9.42; Cl, 5.21; Zn, 9.61. Found: C, 52.53; H, 4.17; N, 12.42; S, 9.40; Cl, 5.28; Zn, 9.79. ^{1}H NMR (DMSO, 298 K, TMS): δ = 2.45 [s, 3 H, Me(pz)], 3.81 (s, 6 H, OMe), 6.10 [s, 1 H, H(pz)], 6.90–7.92 ppm [m, 17 H, H(im) + Ar]. IR (KBr): ν (cm^{-1}): 3482 (br, w), 2933 (w), 2523 (w, B-H), 1598 (w), 1567 (w), 1499 (w), 1462 (w), 1425 (w), 1375 (w), 1278 (w), 1244 (w), 1180 (w), 1093 (w), 1015 (w), 763 (w), 729 (w), 689 (w), 578 (w), 532 (w).

2.2.2. Synthesis of {[HB(Pz^{MePh})(Tt^{OMe})$_2$]ZnClO$_4$} 2

A solution of K[HB(Pz^{MePh})(Tt^{OMe})$_2$] (618 mg, 1.0 mmol) in 50 mL of MeOH was slowly added drop wise (30 min) to a solution of anhydrous Zn(ClO$_4$)$_2$·6H$_2$O (410 mg, 1.1 mmol) in 30 mL of methanol. The resulting precipitate was filtered off. The filtrate was reduced to 20 mL, producing a white precipitate, washed with ether, and finally dried under vacuum. Anal. for C$_{30}$H$_{28}$BClN$_6$O$_6$S$_2$Zn (744.35): Calcd.: C, 48.41; H, 3.79; N, 11.29; S, 8.61; Cl, 4.76; Zn, 8.78. Found: C, 48.76; H, 3.68; N,

11.43; S, 8.60; Cl, 4.70; Zn, 8.87. ^{1}H NMR (DMSO, 298 K, TMS): $\delta = 2.46$ [s, 3 H, Me(pz)], 3.83 (s, 6 H, OMe), 6.12 [s, 1 H, H(pz)], 6.89–7.93 ppm [m, 17 H, H(im) + Ar]. IR (KBr): ν (cm^{-1}): 3492 (br, w), 2834 (w), 2553 (w, B-H), 1611(w), 1503(w), 1466 (w), 1429(w), 1375(w), 1284(w), 1177(w), 1079(vs, ClO$_4^-$), 921(w), 753 (w), 695 (w), 615 (w), 578 (w), 527 (w), 503 (w).

2.3. Preparation of a bare carbon paste electrode (CPE) and carbon paste modified electrodes

Unmodified carbon paste electrode was prepared by mixing 70% graphite powder and 30 % paraffin wax. Paraffin wax was heated till melting and then, mixed very well with graphite powder to produce a homogeneous paste. The resulted paste was then packed into the end of an insulin syringe (i.d.: 2mm). External electrical contact was established by forcing a copper wire down the syringe. CPE modified with Zn (II) complex was prepared by mixing 60% graphite powder and 30% paraffin wax with 1,2,3,4,5,6 and 10% of the complexes, which have been prepared in the previous step. The surface of the electrode was polished with a piece of weighting paper and then rinsed with distilled water thorough.

2.4. Electrochemical Measurements

Cyclic voltammetry (CV) and square wave voltammetry were performed using an Autolab potentiostat PGSTAT 302 (Eco Chemie, Utrecht, The Netherlands) driven by the General purpose Electrochemical systems data processing software (GPES, software version 4.9, Eco Chemie). Electrochemical cell with three electrodes was used; unmodified carbon paste electrode or carbon paste electrode modified with Zinc complexes was used as a working electrode, Ag/AgCl was used as a reference electrode while platinum wire was used as a counter electrode.

2.5. Geometry Optimization and Structure Characterization

Gaussian 03 program was used for all calculations.

3. RESULTS AND DISCUSSION

3.1. Characterization of the zinc model complexes

The tripod ligand K[HB(Pz^{MePh})(Tt^{OMe})$_2$] found to be a good template for getting structural zinc(II) model complexs [20-23]. The synthesis of the chloro and perchlorato zinc complexes [HB(Pz^{MePh})(Tt^{OMe})$_2$ZnCl] **1** and [HB(Pz^{MePh})(Tt^{OMe})$_2$ZnClO$_4$] (2) (Scheme 2) were carried out in abs. methanol by the reaction of the ligand K[HB(Pz^{MePh})(Tt^{OMe})$_2$] with equimolar amount of the ZnCl$_2$ or Zn(ClO$_4$)$_2$·6H$_2$O under anaerobic conditions. The substitution at 3- and 5- positions of the pyrazolyl ring is required for stabilizing the obtained compounds **1** and **2**. The unsubstituted tris(pyrazolyl)borate has led to the formation of the octahedral [HB(Pz)$_3$]$^-$ [24].

$$\{[HB(Pz^{MePh})(Tt^{OMe})_2]ZnX\}$$

$$X = Cl \qquad (1)$$

$$ClO_4 \quad (2)$$
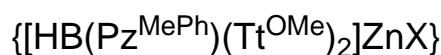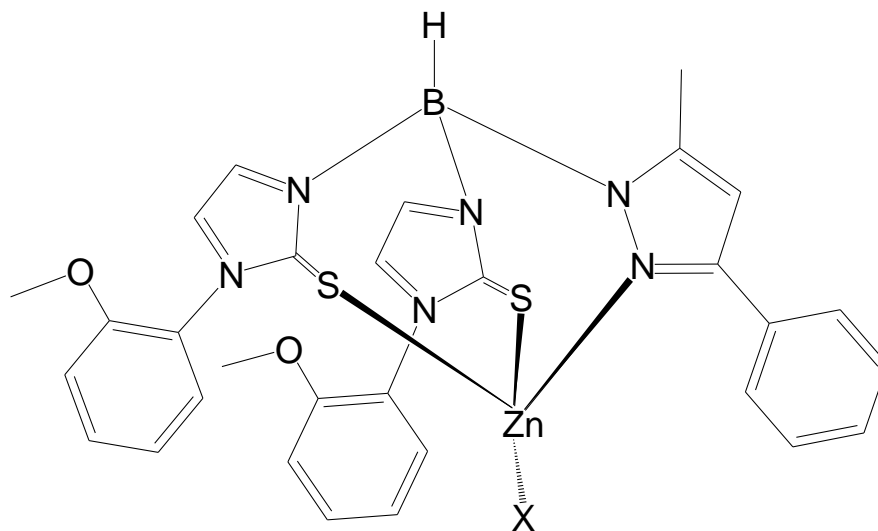
Scheme 2. The structures of the ligands and their zinc(II) model complexes **1** and **2**

This usually results in a preference for the tetrahedral geometry over the octahedral one. The spectral data showed that **1** and **2** have 1:1 stoichiometry. They are stable in both solid and in solution under the atmospheric conditions. Both complexes are neutral with low molar conductance values, suggesting that both the chloride and perchlorate anions are coordinated directly to the zinc ion in solution. On the basis of the literature survey as well as the obtained spectral results, the coordination geometries of both complexes are suggested to be tetrahedral.

3.1.1. IR spectra of the model complexes

The IR spectral data of the ligand $K[HB(Pz^{MePh})(Tt^{OMe})_2]$ gave voluble information about its binding sites to the zinc ion. The formation of **1** and **2** is evidenced from the presence of a v(B-H) stretching band in the range of 2523-2553 cm^{-1}. This band, which appears at 2446 cm^{-1} in the ligand $K[HB(Pz^{MePh})(Tt^{OMe})_2]$, shifts to higher energy in complexes **1** and **2**. A similar shift has previously been reported in Tp complexes [25]. The spectrum showed other bands assigned to the stretching v(C-H) and v(C=N) as well as the bending δ(C-H). Additionally, both complexes appeared weak bands at 442, 449, and 452 cm^{-1}, which indicating the existence of M–N bond. The perchlorate complex **2** shows very intense bands at 1079 and 753 cm^{-1}, indicating the binding character of ClO_4^- [26]. In the v(C-H) stretching region, very broad absorption bands extending from about 3482 to 3492 cm^{-1} are detected for the lattice water molecules in both complexes [27].

3.1.2. Thermal analysis of the model complexes

The decomposition of the chloride complex **1** proceeds in several stages. The complex was found to be stable up to 250 °C. Then a continuous mass loss occurs from 250 to 880 °C with three endothermic events, accompanied by a mass loss of 89.90% (calc. 89.43%). This was assigned to the decomposition of both the chlorine atom and the organic part, forming zinc powder (Found 10.10%; Calc. 10.57%).

3.2. Geometry Optimization and Structure Characterization

Gaussian 03 program wasfor the calculation. Density functional theory (DFT) using B3LYP method and 6-311++G(d,p) basis set was used for structural optimization and frequency calculations [28]. In order to verfiy the stationary points on the potential energy surface, analytical frequency calculations were performed.
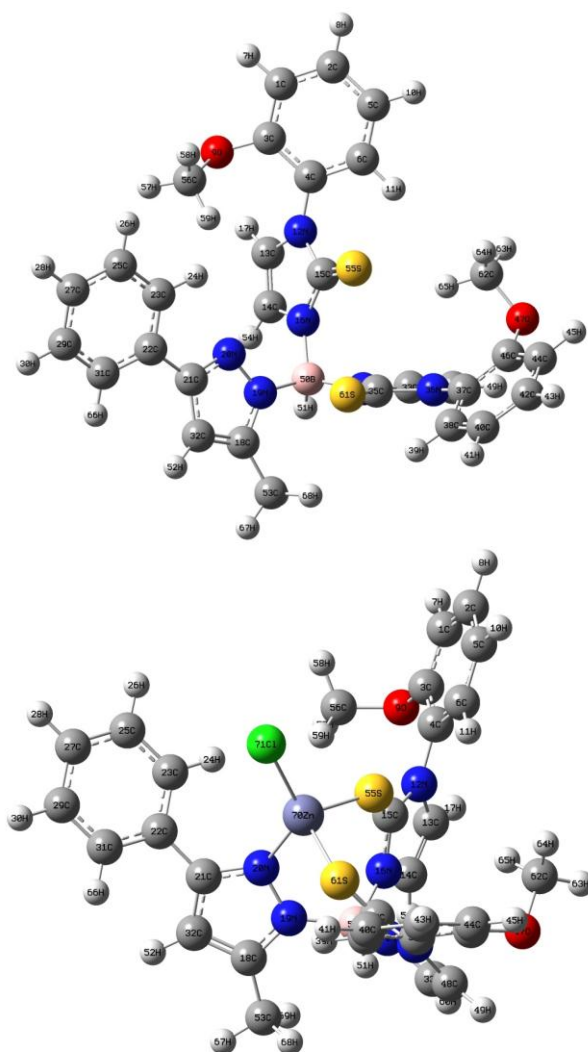

Figure 1. Ball and stick models of the optimized geometry of (a) the ligand K[HB(Pz^{MePh})(Tt^{OMe})$_2$ and (b) zinc(II) complex **1**

Only positive frequencies were observed on the potential energy surface, which prove the stability of the optimised structures.
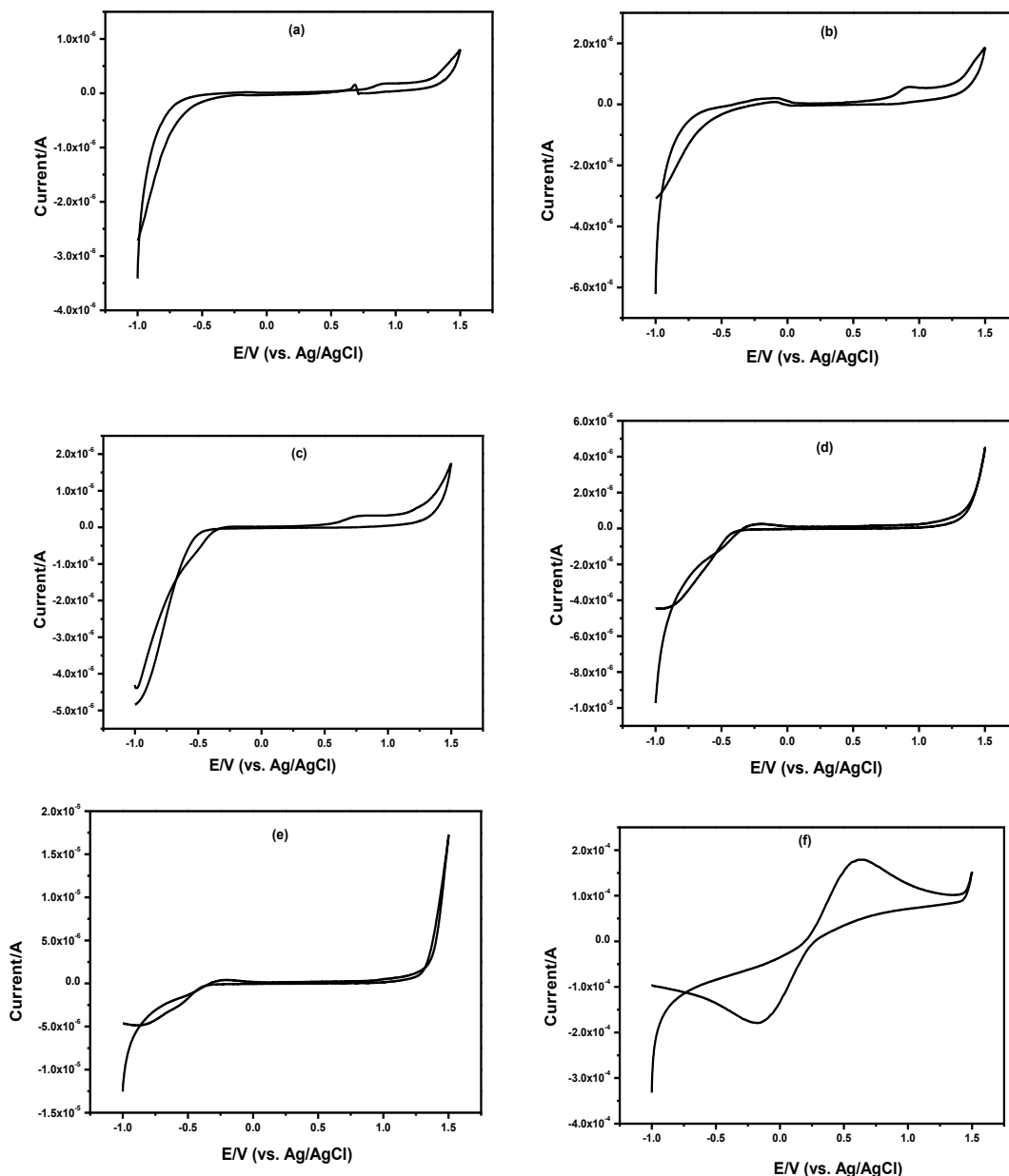

Figure 2. Cyclic voltammograms for a carbon paste electrode modified with $[HB(Pz^{MePh})(Tt^{OMe})_2ZnCl]$ **1** in Britton-Robinson buffer at different pH values using 50 mV/s scan rate. a) pH 3, b) pH 5, c) pH 7, d) pH 9 and e) pH 11. f) showed the cyclic voltammogram for 5.0 mM $K_3[Fe(CN)_6]/K_4[Fe(CN)_6]$ in 0.01 M KCl at carbon paste electrode modified with N_2S +ZnCl$_2$ complex using 100 mV/s (25 ^{o}C).

The optimized geometry structure of the ligand $K[HB(Pz^{MePh})(Tt^{OMe})_2$ is shown in Figure 1a. The DFT calculations, B3LYP/6-311++G(d,p), shows that the uncomplexed ligand stabilized by two hydrogen bonds between the H11 and S55 (2.47 Å, S55…H11−C8 = 107°) and S55 and H65 (2.53 Å,

S55…H65−C62 = 152.2°). Upon complexation of the ligand K[HB(Pz^{MePh})(Tt^{OMe})$_2$ with Zn(II), the tetrahedral complex is formed (Figure 1b). The distance between Zn70 atom and N20 is 2.07 Å (29.6 % shorter than the sum of VDW radius), while the distance between Zn70 atom and S55 is 2.03 Å (30.1 % shorter than the sum of VDW radius). On the other hand, the Zn70 atom is bonded with S61 (Zn70…S61 bond length is 2.02 and bond angle is 115.1). the coordinated Zn atom is bonded with chloride ion by covalent bond (Zn….Cl is 2.19, 30.3 % less than the sum of VDW radius).

3.3. Cyclic voltammetric Studies

Cyclic voltammetry (CV) has become an important electroanalytical technique and widely used in different areas of chemistry. It is widely used to study the redox processes to understand the reaction intermediates, and to obtain information about the stability of reaction products [29].

3.3.1.Carbon paste electrode modified with [HB(Pz^{MePh})(Tt^{OMe})$_2$ZnCl] 1

The electrochemistry for carbon paste electrode modified with [HB(Pz^{MePh})(Tt^{OMe})$_2$ZnCl] **1** was studied using cyclic voltammetry at different ph values (figure 2).

At pH 3 ,5 and 7 only one anodic peak was appeared at +0.9V +0.9 and +0.76V respectively. At pH 9 and 11 one quasi-reversible redox system was appeared. At pH 9 the anodic peak was appeared at -0.25 and the cathodic wave appeared at -0.8V. While at pH 11 the anodic peak was appeared at -0.26 and the cathodic wave appeared at -0.78V. The electrocatalytic activity of carbon paste electrode modified by **1** was examined by cyclic voltammetry in the presence of 5.0 mM K$_3$[Fe(CN)$_6$]/K$_4$[Fe(CN)$_6$]. Figure 2f showed a well quasi- reversible redox system [30], a well-defined anodic peak E$_{pa}$ appeared at +0.63 V and a well cathodic peak E$_{pc}$ at -0.16V. The separation of the anodic and cathodic peak potentials (ΔE) was found < 0.79 V corresponding to Fe(II)/Fe(III) couple [31]. The formal potential E$_{1/2}$ was taken as the average of E$_{pc}$ and E$_{pa}$ is + 0.235 V.

3.3.2.Carbon paste electrode modified with[HB(Pz^{MePh})(Tt^{OMe})$_2$ZnClO$_4$ 2

The electrochemical behavior for a carbon paste electrode modified with [HB(Pz^{MePh})(Tt^{OMe})$_2$ZnClO$_4$] **2** using cyclic voltammetry was shown in figure 3. At pH 3, 5 and 7 only one anodic peak was appeared at +0.9V +0.91 and +0.76V respectively. At pH 9 and 11 one quasi-reversible redox system was appeared. At pH 9 the anodic peak was appeared at -0.27 and the cathodic wave appeared at -0.7V. While at pH 11 the anodic peak was appeared at -0.17 and the cathodic wave appeared at -0.76V. The electrocatalytic activity of carbon paste electrode modified by **2** was examined using cyclic voltammetric technique.
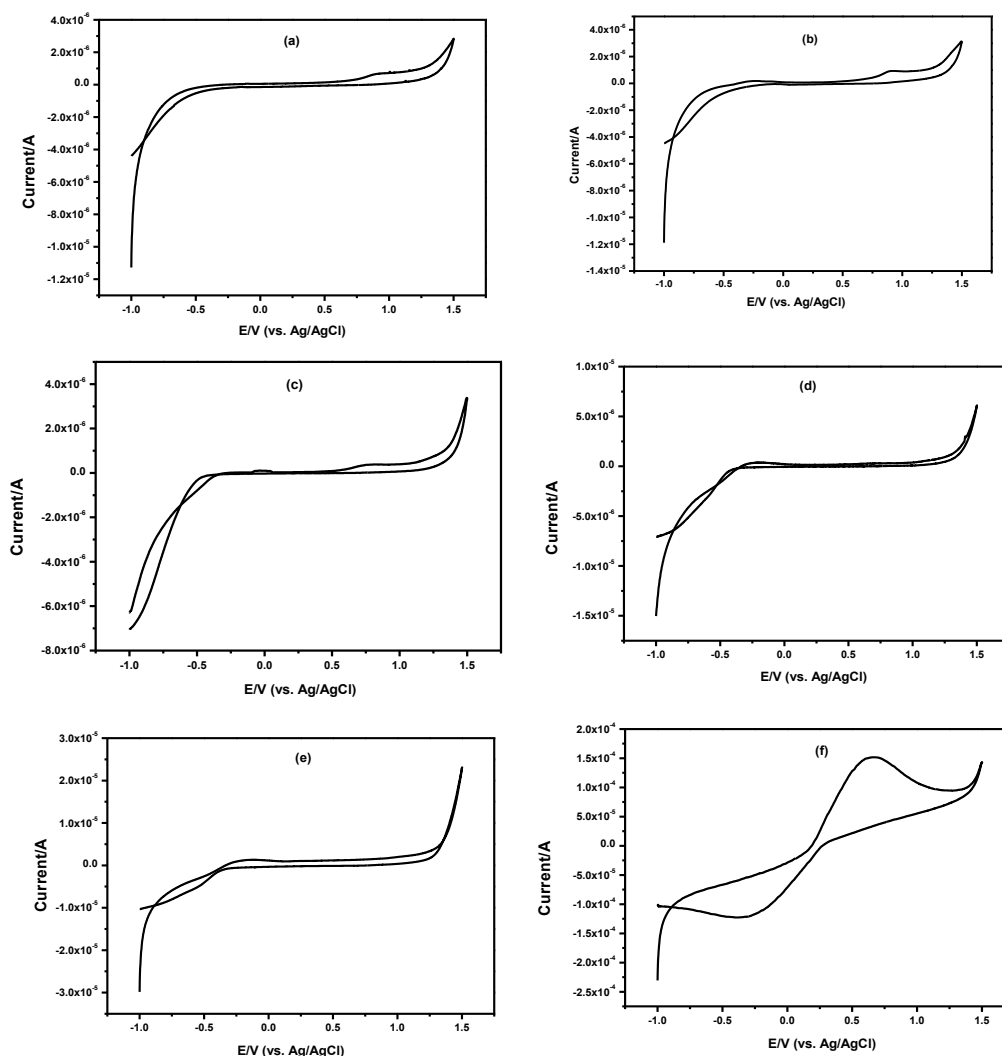
Figure 3. Cyclic voltammograms for a carbon paste electrode modified with [HB(Pz^{MePh})(Tt^{OMe})$_2$ZnClO$_4$] **2** in Britton-Robinson buffer at different pH values using 50 mV/s scan rate. a) pH 3, b) pH 5, c) pH 7, d) pH 9 and e) pH 11. f) showed the cyclic voltammogram for 5.0 mM K$_3$[Fe(CN)$_6$]/K$_4$[Fe(CN)$_6$] at carbon paste electrode modified with N$_2$S +Zn(ClO$_4$)$_2$ complex using 100 mV/s (25 ^{o}C).

Figure 4f showed a well quasi- reversible redox system, a well-defined anodic peak E$_{pa}$ appeared at +0.63 V and a well cathodic peak E$_{pc}$ at -0.36V. The separation of the anodic and cathodic peak potentials (ΔE) was found < 0.99 V corresponding to Fe(II)/Fe(III) couple. The formal potential E$_{1/2}$ is + 0.135 V.

3.4. Electrochemistry of P-ntrophenol (PNP)

The hydrolysis of organophosphorus compounds using hydrolase enzyme will generates *p*-nitrophenol, which is electroactive [32]. The organophosphorus hydrolase based amperometric biosensing of organophosphorus compounds relies on the anodic detection of this enzymatically liberated *p*-nitrophenol (PNP) by the electrode [33-35].
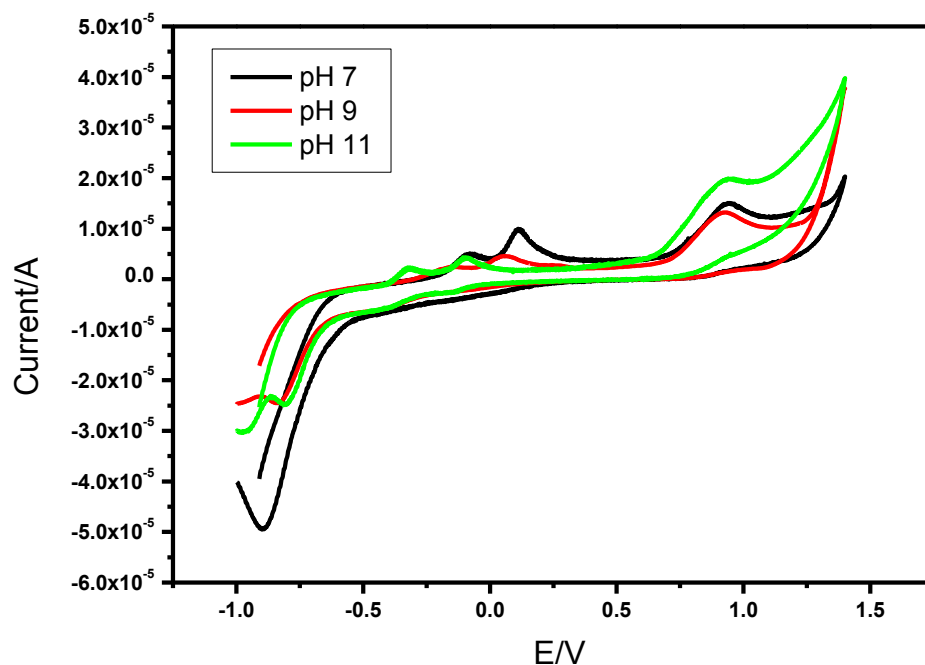
Figure 4. Cyclic voltammograms for CPE in 10 ml BR buffer at pH =7, 9 and 11 after the addition of 4×10^{-5} M PNP, at 100 mV s^{-1} (25 ^{o}C).

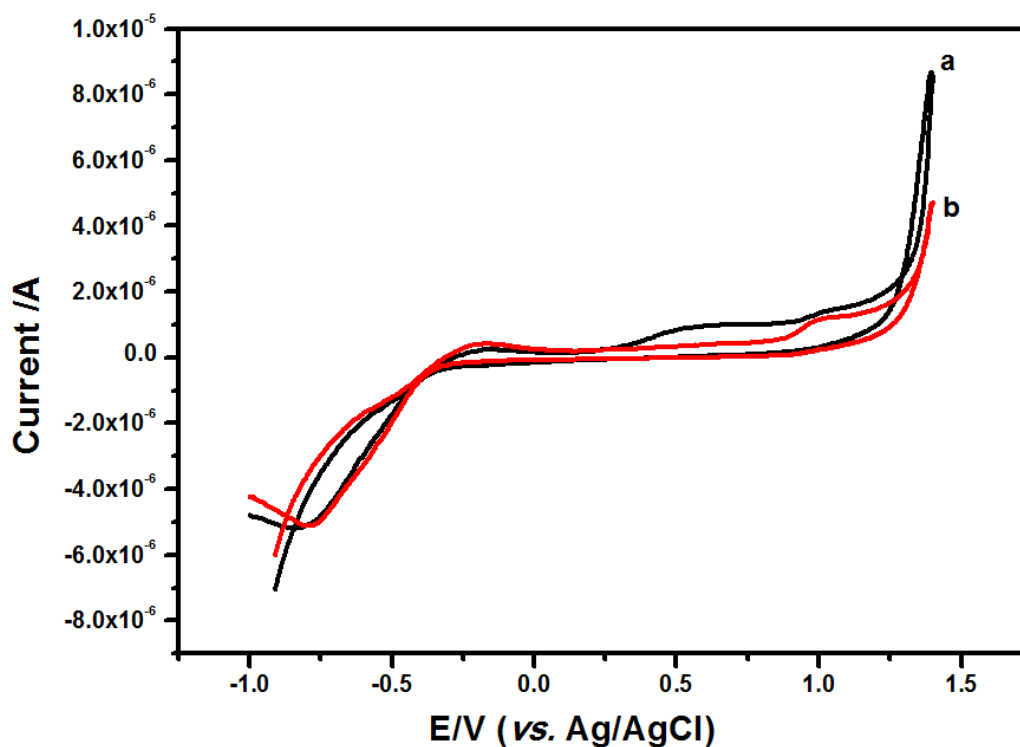**Figure 5.** Cyclic voltammograms for CPE + [HB(Pz^{MePh})(Tt^{OMe})$_2$ZnCl] **1** in 10 ml BR buffer pH =11 in (a) the absence and (b) in the presence of 1×10^{-5} M TPP using 100 mV s^{-1} (25 ^{o}C).

The oxidation current measured at a fixed potential using a potentiostat, is directly proportional to the concentration of PNP formed. To detect the optimum conditions for the electrochemical determination of enzymatically produced PNP, the electrochemistry for PNP was examined using $1x10^{-5}$ M at different pH values (7 , 9 and 11) using BR buffer.

Figure 5 shows the cyclic voltammograms for CPE before and after the addition of $4x10^{-5}$ M PNP using BR Buffer at pH 7. In the absence of PNP, no marked peaks were appeared and after the addition of $4x10^{-5}$ M PNP, three oxidation peaks were appeared at -0.08, +0.11 and +0.95 V due to the oxidation of nitro group. The highest oxidation peak was appeared at +0.95 V. To detect which pH is suitable for the determination of PNP, the cyclic voltammograms for $4x10^{-5}$ M PNP were collected in figure 4. The height oxidation peak was appeared at pH 11 in which will be used for the electrochemical determination of the enzymatically produced PNP.

3.5. Analytical Applications

3.5.1 Electrochemical behavior of TPP at CPE electrode modified by using complexes 1 and 2

The electrochemical behavior of TPP on CPE modified by using complexes **1** and **2** were studied in a potential range from -1.0 to +1.5 V (vs. Ag/AgCl). Figures 5 and 6 show the resulted voltammograms for CPE modified by complexes **1** and **2** in the presence of $1x10^{-5}$ M TPP in BR buffer pH 11. As shown from figure 7, TPP gave one oxidation peak for both complexes at +1.0 and +0.98 V, respectively.
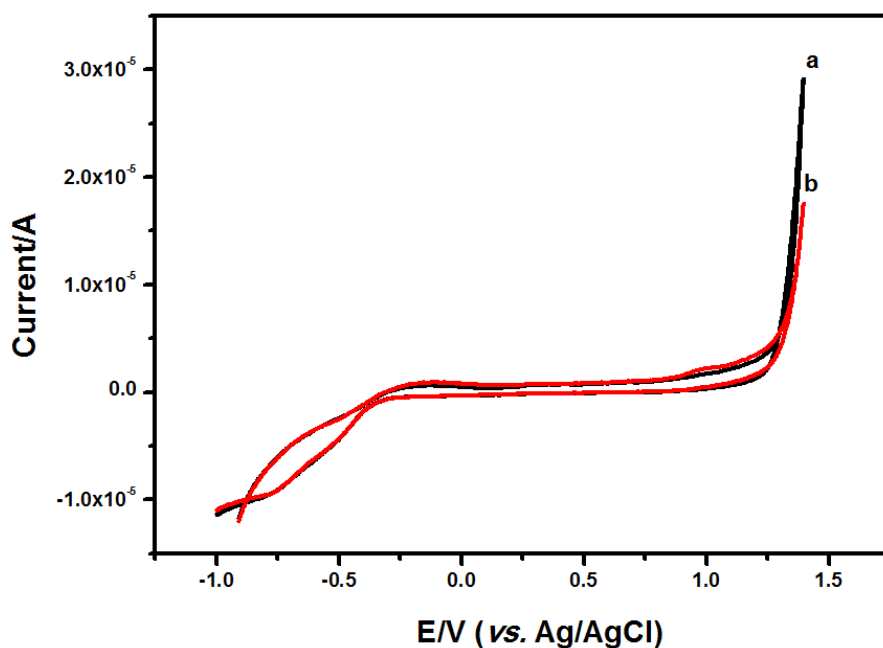

Figure 6. Cyclic voltammograms for CPE + [HB(Pz^{MePh})(Tt^{OMe})$_2$ZnClO$_4$] **2** in 10 ml BR buffer pH =11 in (a) the absence and (b) in presence of $1x10^{-5}$ M TPP using 100 mV s^{-1} (25 ^{o}C).
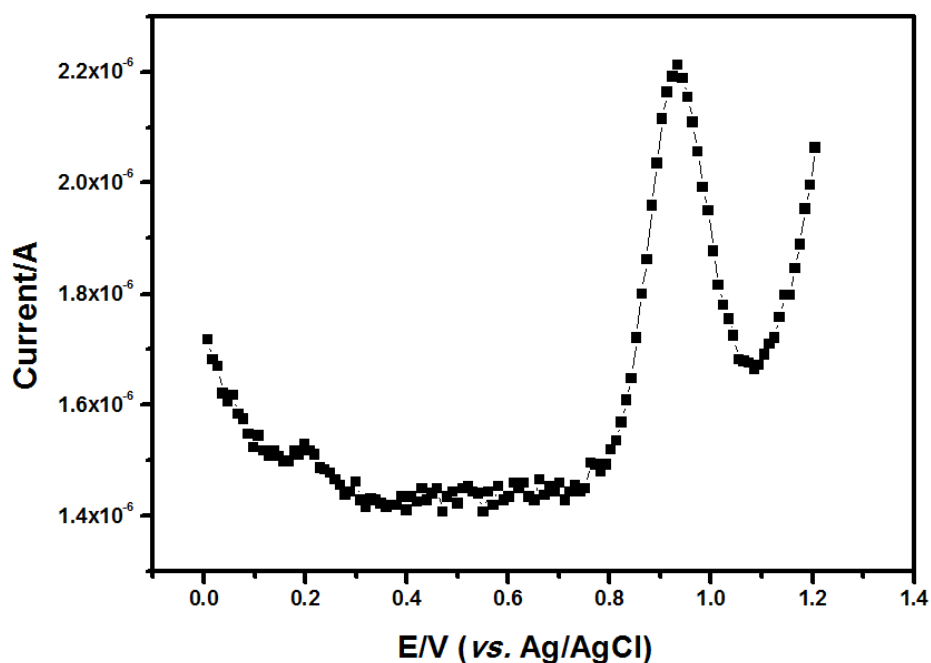
Figure 7. Square wave voltammetry for CPE modified by [HB(Pz^{MePh})(Tt^{OMe})$_2$ZnCl] **1** in 10 ml BR buffer (pH =11) using 4 x10^{-5} M TPP (25 ^{o}C).

3.5.2. Electrochemical determination of TPP at CPE modified electrodes by using complexes 1 and 2
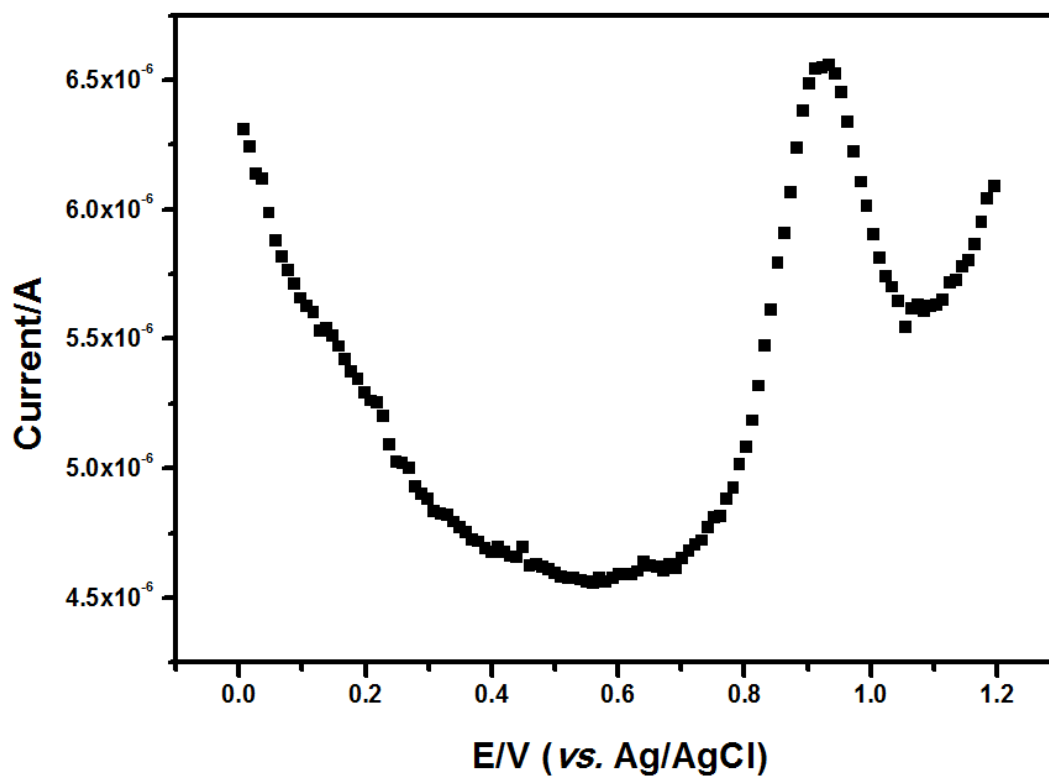

Figure 8. Square wave voltammetry for CPE modified by [HB(Pz^{MePh})(Tt^{OMe})$_2$ZnClO$_4$] **2** in 10 ml BR buffer (pH =11) using 1 x10^{-4} M TPP (25 ^{o}C).

The triphosphate TPP was detected using carbon paste electrode modified with both **1** and **2**. TPP showed one oxidation peak using BR buffer (pH 11) using square wave voltammetry at +0.93 and +0.93 V for **1** and **2**, respectively (figure 8).

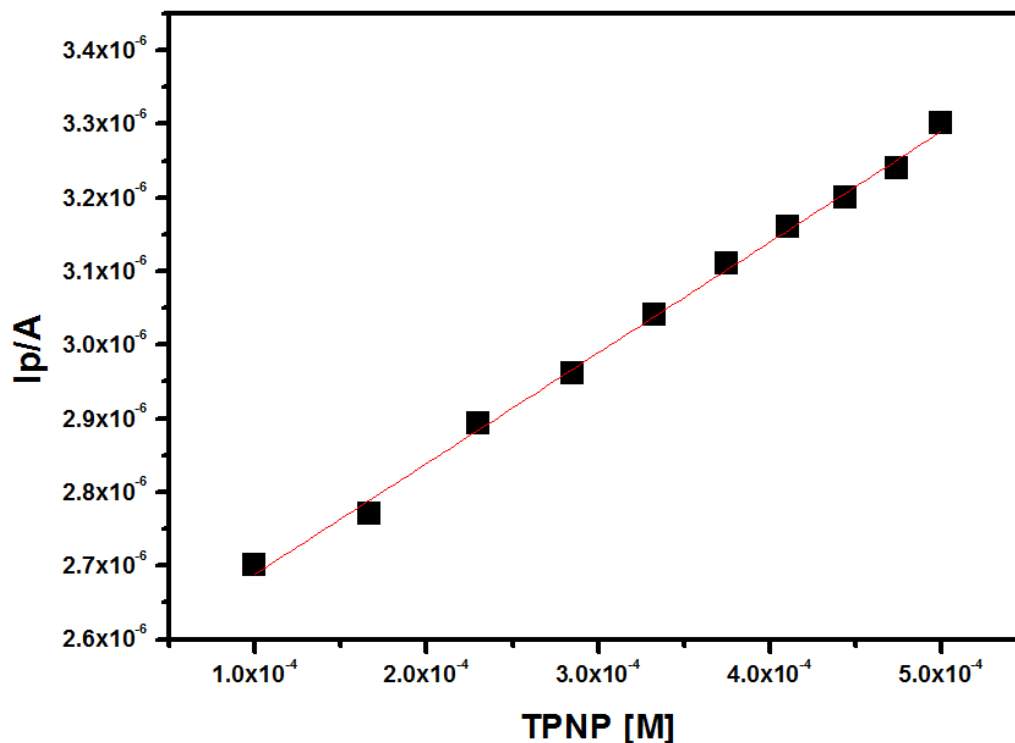### 3.5.3. Calibration Curve and Limit of detection:

Figure 9. The effect of TPP concentration (from $1x10^{-4}$ to $1x10^{-3}$ M) on the response of CPE modified by [HB(Pz^{MePh})(Tt^{OMe})$_2$ZnCl] **1** using square wave voltammetry at in 10 ml BR buffer (pH =11) (25 ^{o}C).

The TPP was detected using CPE electrode modified by [HB(Pz^{MePh})(Tt^{OMe})$_2$ZnCl] **1** complex using square wave voltammetric technique. By increasing TPP concentration, the peak current signals for square wave voltammograms increased. The effect TPP concentration on the peak current was examined from $1x10^{-4}$ M to $1x10^{-3}$ M, the resulted calibration curve showed a linear behavior with a correlation coefficient of 0.9987 and a relative standard deviation (RSD) of 1.095×10^{-8} (figure 9).

The detection limit is lowest amount of analyte present in sample that can be detected but not necessarily quantities, under stated condition. The lower detection limits for TPP was calculated based on the standard deviation of the response (SD) and the slope of the calibration curve (m) at levels approximating the LOD according to the formula: LOD = 3(SD/m) and it was found to be 2.19×10^{-5} M.

The triphosphate TPP was detected also by using CPE electrode modified by [HB(Pz^{MePh})(Tt^{OMe})$_2$ZnClO$_4$] **2** using square wave voltammetric technique. By increasing TPP concentration, the peak current signals for square wave voltammograms increased. The effect TPP concentration on the peak current was examined from $1x10^{-4}$ M to $1x10^{-3}$ M, the resulted calibration

curve showed a linear behavior with a correlation coefficient of 0.994 and a relative standard deviation (RSD) of 4.344×10^{-8} (figure 10).
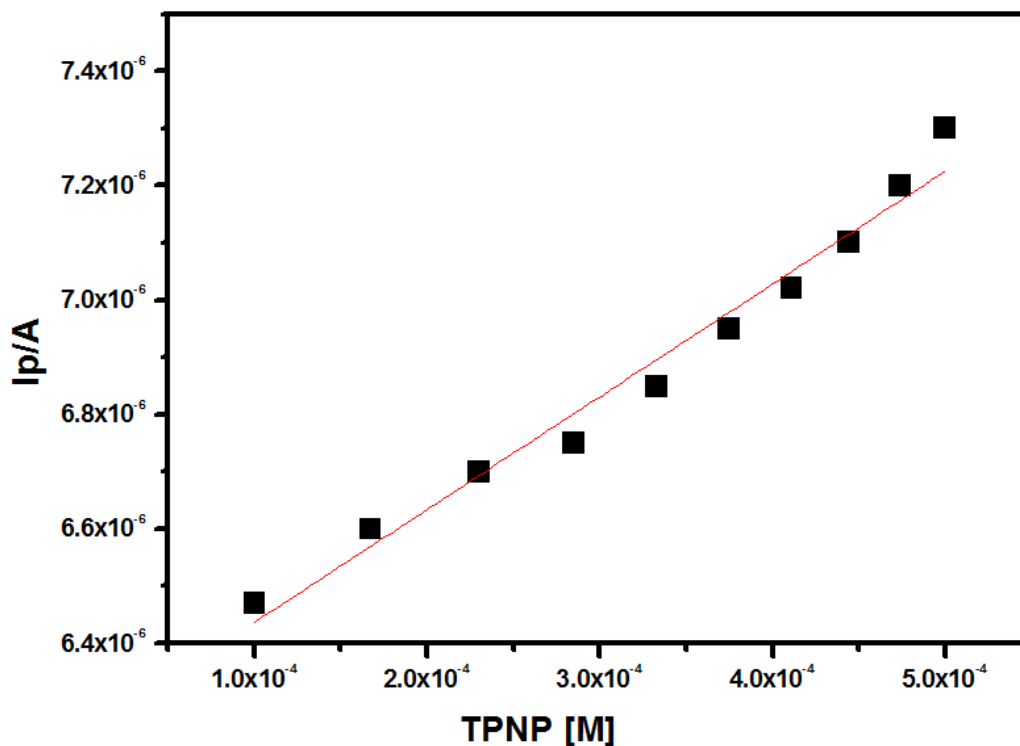

Figure 10. The effect of TPP concentration (from 1×10^{-4} to 1×10^{-3} M) on the response of CPE modified by $[HB(Pz^{MePh})(Tt^{OMe})_2ZnClO_4]$ **2** using square wave voltammetry at in 10 ml BR buffer (pH =11) (25 °C).

The lower detection limits for TPP was calculated based on the standard deviation of the response (SD) and the slope of the calibration curve (m) at levels approximating the LOD according to the formula: LOD = 3(SD/m) and it was found to be 6.61×10^{-5} M. The obtained LOD for TPP was compared with the previous work in Table 1.

Table 1. The obtained LOD for TPP in our method and other works.

Technique	Electrode	Concentration Detected [M]	Reference
Linear sweep voltammetry	screen printed gold electrode	2.0×10^{-6}	36
Linear sweep voltammetry	screen printed gold electrode	1.6×10^{-5}	6
Square wave voltammetry	CPE electrode modified by $[HB(Pz^{MePh})(Tt^{OMe})_2ZnCl]$ **1**	2.19×10^{-5}	This work
Square wave voltammetry	CPE electrode modified by $[HB(Pz^{MePh})(Tt^{OMe})_2ZnCl]$ **2**	6.61×10^{-5}	This work

4. CONCLUSION

In this work a new biomimetic sensors were prepared by modification of carbon paste electrode with $[HB(Pz^{MePh})(Tt^{OMe})_2]^-$ Zn(II) complexes as structural mimics for the active site of *hydrolase (phosphotriestrase)* enzyme. The obtained zinc(II) model complexes have been characterized by IR and thermal analysis. The electrochemical behavior of the prepared biomimetic sensors has been studied by using cyclic voltammetry (CV). The electrochemical behavior of tris(p-nitrophenyl)phosphate (TPP) has been studied using cyclic and square wave voltammetric techniques at the prepared biomimetic sensors. TPP was electrochemically detected using square wave voltammetry. Using a biomimetic sensor prepared by modification of carbon paste electrode with zinc(II) complex **1**, a linear behavior for TPP was obtained in a concentration range from 1×10^{-4} M to 1×10^{-3} M, with a correlation coefficient of 0.9987 and a relative standard deviation (RSD) of 1.095×10^{-8}. While by using complex **2** as model for hydrolase enzyme a linear behavior for TPP was obtained in a concentration range from 1×10^{-4} M to 1×10^{-3} M, with a correlation coefficient of 0.994 and a relative standard deviation (RSD) of 4.344×10^{-8}. The detection limit obtained using carbon paste electrode modified by complex **1** and **2** was to be 2.19×10^{-5} M and 6.61×10^{-5} M, respectively.

References

1. H. Coates, *Ann. Appl. Biol*. 36 (1949) 156
2. D. J. Ecobichon. In Casarett and Doull's Toxicology: The Basic Science of Poisons, 4th ed.; M. O. Amdur, J. Doull, C. D. Klaasen, Eds.; McCraw-Hill: New York (1991) 565
3. O. Li-Tse and A. Sharma, *J. Agric. Food Chem*. 37 (1989) 1514
4. M. M. Ibrahim, G. A. M. Mersal, *J. Inorg. Biochem*. 104 (2010) 1195
5. M. M. Ibrahim, *J. Mol. Struct*. 990 (2011) 227-236
6. M. M. Ibrahim, G. A. M. Mersal, *International Journal of Electrochemical Science*, 8 (2013) 1328
7. M. M. Ibrahim, G. A. M. Mersal, H. Shokry, *International Journal of Chemical Engineering* 30 (2013) 2051
8. G. A. M. Mersal, M. M. Ibrahim, *Comptes Rendus Chimie* 15 (2012) 336
9. M. Ibrahim, A. M. Ramadan, *J. Incl. Phenom. Macrocycl. Chem.* 72 (2012) 103
10. M. M. Ibrahim, M. A. Ramadan, *J. Incl. Phenom. Macrocycl. Chem*. 68 (2010) 287
11. M. M. Ibrahim, H. A. Eissa, G. E. Kamel, and H. Y. El-Baradie, Synthesis and Reactivity in Inorganic, *Metal-Organic, and Nano-Metal Chemistry*. 40 (2010) 869
12. M. M. Ibrahim, K. Nakata, K. Ichikawa, 23th Symposium on Solution Chemistry, Institute for Molecular Science (IMS), 11, 2000, 16-18, Nagoya (Higashi Okazaki), Japan.
13. M. M. Ibrahim, *J. Inorg. Organomet. Polym*. 19 (2009) 532
14. T. Echizen, M. M. Ibrahim, K. Nakata, M. Izumi, K. Ichikawa, M. Shiro, *J. Inorg. Biochem*. 98 (2004) 1347
15. M. M. Ibrahim, K. Ichikawa, M. Shiro, *Inorg. Chim. Acta* 535 (2003) 187.
16. M. M. Ibrahim, N. Shimomura, K. Ichikawa, M. Shiro, *Inorg. Chim. Acta* 313 (2001) 125
17. L, Viala, P. Dumy, *New J. Chem.*, 33 (2009) 939
18. S. Fletcher, A. D. Hamilton, *Journal of The Royal Society Interface* 3, (2006) 215
19. M. Kruppa, B. König, *Chem. Rev*. 106 (2006) 3520
20. M. Ruf, K. Weis, H. Vahrenkamp, *H. J. Am. Chem. Soc*. 118 (1996) 9288-9294.

21. M. M. Ibrahim, G. He, J. Seebacher, B. Benkmil, H. Vahrenkamp, *Eur. J. Inorg. Chem.* (2005) 4070
22. M. Shu, R. Walz, B. Wu, J. Seebacher, H. Vahrenkamp, *Eur. J. Inorg. Chem.* (2003) 2502
23. H. Vahrenkamp, Coordination chemistry of zinc related to an understanding of its biological functions. In Bioinorganic Chemistrys Transition Metals in Biology and their Coordination Chemistry; Trautwein, A. X., Ed.; Wiley-VCH: Weinheim, (1997) 540
24. S. Trofimenko, J. C. Calabrese, J. S. Thompson, *Inorg. Chem.*, 26 (1987) 1507
25. C. Eicken, B. Krebs, J. C. Sacchettini, *Curr. Opin. Struct. Biol.* 9 (1999) 677
26. W. H. Habig, M. J. Pabst, W. B. Jakoby, *J. Biol. Chem.* 249 (1974) 7130.
27. H. Takeuchi, I. Harada, *Spectrochim. Acta* 42A (1986) 1069
28. A. k. Pandey, A. K. Bajpai, A. Kumar, M. Pal, V. Baboo, A. Dwivedi, *J. Theor. Chem.* 2014 (2014) 1
29. D. D. Moulton, R. Farid, A. J. Bard, *J. Electroanal. Chem.* 256 (1988) 309
30. R. R. Zhuang, F. F. Jian, K. Wang, *Cent. Eur. J. Chem.* 8 (2010) 646
31. H. M. Carapuça, M. S. Balula, A. P. Fonseca, A. M. V. Cavaleiro, *J. Solid State Electrochem.* 10 (2006) 10
32. A. Mulchandani, W. Chen., P. Mulchandani, J. Wang, K. R Rogers, *Biosensors and Bioelectronics* 16 (2001) 225
33. J. H. Lee, J. Y. Park, K. Min, H. J. Cha, S.S. Choi, Y. J. Yoo, *Biosensors and Bioelectronics* 25 (2010) 1566
34. M. Stoytcheva, R. Zlatev, V. Gochev, Z. Velkova, G. Montero, *Anal. Methods* 6 (2014) 8232.
35. B. Prieto-Simón, M. Campàs, S. Andreescu, J. Marty, *Sensors* 6 (2006) 1161
36 M.M. Ibrahim, Gaber A. M. Mersal, *J Inorg Organomet Polym* 19 (2009) 549